Testing of Atmospheric Turbulence Effects on the Performance of Micro Air Vehicles

David Lundström and Petter Krus

Linköping University Post Print

N.B.: When citing this work, cite the original article.

Original Publication:

David Lundström and Petter Krus, Testing of Atmospheric Turbulence Effects on the Performance of Micro Air Vehicles, 2012, INTERNATIONAL JOURNAL OF MICRO AIR VEHICLES, (4), 2, 133-149.

http://dx.doi.org/10.1260/1756-8293.4.2.133

Copyright: Multi-Science Publishing

http://www.multi-science.co.uk/

Postprint available at: Linköping University Electronic Press http://urn.kb.se/resolve?urn=urn:nbn:se:liu:diva-81837

Testing of Atmospheric Turbulence Effects on the Performance of Micro Air Vehicles

David Lundström and Petter Krus Linköping University, Department of Management and Engineering 58183 Linköping, Sweden

Email: david.lundstrom@liu.se / petter.krus@liu.se

ABSTRACT

Micro Air Vehicles (MAV) are generally operated at low altitudes and within the earth boundary layer. This is a very dynamic environment with varying wind intensity and turbulence levels far greater than those experienced by traditional manned aircraft cruising at higher altitudes. Yet aerodynamic research on MAVs is often based on the assumption of steady aerodynamics. Little effort has been made to experimentally determine the validity of this assumption. In this paper, the effect of turbulence on the performance of a MAV is studied using flight testing in different wind conditions. Flight testing technique, data logging equipment and data reduction are explained. Additionally, a low cost technique for propeller performance measurement is presented. Results show that the flow around a MAV flying in windy conditions qualifies as highly unsteady, although the impact on its performance is surprisingly small for the kind of turbulence levels at which MAVs can be expected to operate. Accelerometer data from the flights reveals that if steady aerodynamic theory is assumed, increasing turbulence should have resulted in a measurable drag increase, thus indicating that the tested MAV to some extent passively manages to benefit from the turbulence.

NOMENCLATURE

AR	Aspect Ratio	L	Lift
c	Wing chord	n	Propeller revolutions per second
C_D	Drag coefficient	Ω	Propeller radians per second
C_{D_0}	Zero lift drag coefficient	P	Power
C_{D_i}	Lift induced drag coefficient	$R_{0.75}$	Propeller ¾ radius length
C_L	Lift coefficient	S	Wing reference area
C_P	Propeller power coefficient	T	Thrust
C_T	Propeller thrust coefficient	v	Free stream velocity
D	Drag	v_{Re}	Propeller Reynolds number velocity
d	Propeller diameter	ho	Air density
J	Advance ratio	ω	Angular frequency
k	Reduced frequency parameter	η	Efficiency

1. INTRODUCTION

The atmospheric boundary layer (ABL) is the region of air affected by the friction between the surface of earth and the wind. It results in a gradient wind field within which the air flow is complex and turbulent. The characteristics of the ABL depend on the underlying terrain and atmospheric conditions. Over flat uniform terrain it typically extends to a height of 500-1000 meters above the ground [1]. MAVs normally operate in the lower region of this envelope, where the turbulence intensity is very strong, and atmospheric turbulence must therefore always be expected to impact MAV aerodynamics. The characteristics of the atmospheric boundary layer have been well studied in the past in the field of meteorology and wind engineering [1-3]. More recent studies have explored the characteristics of the ABL very close to the ground and with direct application to MAVs [4].

The practical implications of a MAV flying in turbulence is, most obviously, that its attitude

and flight path will be disturbed. Turbulence or wind gusts will induce unwanted pitch, roll and yaw inputs and trigger dynamic responses such as phugoid, short period and Dutch roll oscillations [5]. Most research regarding the effect of atmospheric turbulence on MAVs is targeted towards understanding and minimizing these unwanted responses, with the goal of making MAVs into as stable of sensor platforms as possible.

An area that has been paid less attention is the effect of atmospheric turbulence on aerodynamic performance. There are several reasons why turbulence would be expected to influence both lift and drag properties. The constant attitude changes and excitation of oscillatory modes need to be either corrected by the control system or dampened by the aerodynamic stability inherent in the design. This results in extra drag. Moreover, the rapid fluctuations in flow direction in the ABL have the potential to profoundly affect the aerodynamics of the vehicle. Measurements by Watkins et al [4], taken 2 meters above the ground in 4 m/s wind, illustrate the complex nature of the flow in the ABL (Figure 1).

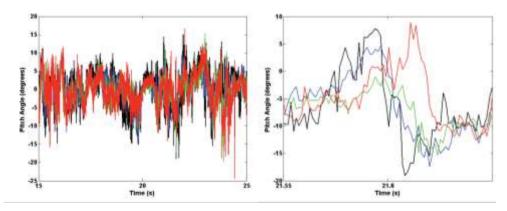


Figure 1. Pitch angle variation in 4 m/s wind measured by four probes with 150 mm lateral separation and at an elevation of 2 m, from Watkins et al [4], with permission.

For such rapid flow fluctuations, traditional stationary aerodynamic theory is invalid. At higher altitudes and at typical flying speeds the variations in pitch angle will be less pronounced but it is still likely that the aerodynamics of MAVs flying in the lower regions of the ABL will qualify as unsteady. Assumptions regarding lift and drag made during design may not be valid. As long ago as 1922 Katzmayr [6] showed that an oscillating airflow considerably altered the aerodynamic properties of airfoils. His results showed that the average drag as a function of average lift could increase as well as decrease depending on the conditions. The latter is often referred to as the Katzmayr effect. Even though this is established knowledge, aerodynamic research on MAVs is often based on the assumption of stationary flow. For instance, traditional wind tunnels do not replicate the turbulent environment representative of the real world atmosphere [7]. Yet it is the common tool for experimental MAV research. Similarly, in CFD simulations the common assumption is that the inflow is smooth and uniform.

With the above considerations in mind, it was decided to experimentally study to what extent the turbulence within the lower regions of the ABL affects the performance on MAVs. A straightforward approach with flight testing was selected. One of the University MAVs was equipped with data logging equipment and flight-tested in several different ABL conditions with the objective to determine its aerodynamic efficiency. The assumption was that increasing wind and turbulence would result in a noticeable change in performance. In addition to evaluating the relative effect of turbulence, the flight tests was also intended to provide absolute data for latter evaluation of MAV performance prediction methods as part of the authors' on-going research in MAV design automation [8, 9].

Aerodynamic efficiency, i.e. lift to drag, in flight can be measured either by means of a power off glide slope technique or with power on using a thrust-calibrated propulsion system. For turbulent conditions, the power on method is the only feasible method. Performance flight testing, using this technique applied to small electric powered UAVs, has previously been demonstrated by Ostler et al [10]. They calibrated thrust as a function of velocity and motor input power. Considering that electric motor efficiency is coupled to motor temperature [9], it was decided for these tests to use the more common method of calibrating propeller characteristics as a function of rpm and velocity.

2. PROPULSION SYSTEM CHARACTERIZATION

Propeller characteristics are commonly described by the thrust and power coefficients, C_T and C_P , (Equation 1-2) as a function of advance ratio, J, (Equation 3).

$$C_T = \frac{T}{\rho n^2 d^4} \tag{1}$$

$$C_P = \frac{P}{\rho n^3 d^5} \tag{2}$$

$$J = \frac{v}{nd} \tag{3}$$

Ideally, C_T and C_P are only dependent on advance ratio but in reality they are also coupled to Reynolds number and aeroelastic effects such as blade twisting. In order to fully define the C_T and C_P coefficients the propeller's thrust and input power need to be mapped against the entire velocity and rpm range over which it is intended to operate. This is traditionally carried out in wind tunnel testing. Examples of wind tunnel data for typical model hobby propellers can be found at the University of Illinois extensive propeller database [11]. Unfortunately, this database contained no data for propellers small enough to suit the MAV selected for the tests. As a first step, the propeller of the MAV, an APC 6x5.5, had to be tested. With no wind tunnel available an alternative test method was developed. As a wind tunnel substitute a measurement rig was mounted on the roof of a car. The in-house designed test rig is shown in Figure 2. The rig measures thrust and torque using a set of carefully arranged strain gauges. The measurement range is 0-30 N of thrust and 0-0.3 Nm of torque, each sampled at 15 bit resolution. Additionally the rig measures rpm, free stream static and dynamic pressure, air temperature, flow inclination in pitch and yaw using vanes, and, although not required, it also measures the motor current and input voltage. The hardware design for torque and thrust measurement is described in more detail in Ref [12] where it was used to study the characteristics of electric motors and motor controllers.



Figure 2. Car-mounted propeller test rig.

The data logging was performed using an Eagle Tree Systems USB Flight Data Recorder Pro. Together with additional sensors for measuring analog signals and GPS, it offered a convenient off-the-shelf solution for data acquisition. The rig was mounted on top of a sturdy tripod which in turn was mounted on the roof of the car. To minimize the aerodynamic disturbance from the car the tripod places the propeller as high as two meters above the car roof. Both the data logger and

the motor controller were controlled from a laptop placed on the passenger seat. The test procedure consisted of starting the logging, accelerating the car up to a given speed at which the cruise control was activated, and then executing an automatic test sequence that advanced the motor's electronic speed controller (ESC) in steps of 12.5% until 100% power was reached. An example of a data log from such a test is shown in Figure 3.

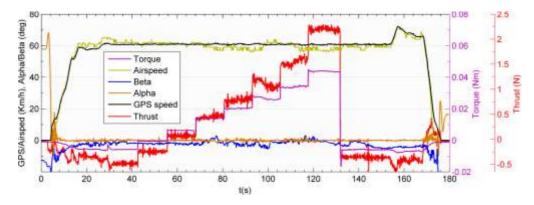


Figure 3. Raw data from propeller car top testing.

During the testing, factors such as wind, vibrations due to road roughness etc induced noise to the measurements. To minimize the effect of this noise, the length of each segment with constant throttle was 13 s. Along with a log frequency of 40Hz, this provided enough data samples to easily filter out the noise. To capture any effects of Reynolds number and potential blade twisting, the test procedure was repeated for 6 different speeds in the range of 40-100 km/h, as well as a static test. The actual testing was carried out on a public road in flat terrain. To avoid traffic and to obtain as low and constant wind conditions as possible, all the testing was performed at night.

In order to simplify the data reduction, a script was written that automatically screened through the data to sort out useful data sections. The script divided the data into segments of 120 data points. Within each segment, the script examined the data to verify that each parameter stayed within predefined min/max values and that no variation larger than the expected noise occurred. If all requirements were met, the data for that segment was averaged and stored in a new dataset. This ensured that for the extracted data, the car was not under acceleration, the throttle did not change, and no sudden changes in flow inclination or pitot pressure occurred. In order to visualize and further validate the results of the data screening, a Google Earth KML file was generated where the GPS trail is coloured depending on the quality of the data. Figure 4 illustrates the KML file from one test. The green colour represents segments of valid data.



Figure 4. GPS trail of propeller test.

At the time of the tests, the weather conditions were what one generally would observe as calm. However, weather services reported a constant breeze of approximately 1.5 m/s in a direction of approximately 45 degrees to the road. This was observed in the data as an inclination of the free stream relative to the propeller shaft, as well as a difference between airspeed and GPS speed. At higher speeds, the flow inclination was negligible but at the minimal tested speed (40km/h) the data log showed inclinations of approx. 8 degrees with peaks up to 11 degrees. When processing the data, considerations were made about what effect the flow inclination would have on the

validity of the pitot tube measurements as well as the thrust and power measurements. The pitot tube range of insensitivity to inclination has not been calibrated, but the design is made following the recommendations made by Gracey [13] and should have an error margin less than 1% for flow inclinations below 10 degrees. No corrections were therefore made to the airspeed measurements.

The effect of flow inclination on thrust and power coefficients have been well studied and documented. Correction methods have been thoroughly described by for instance DeYoung [14]. For inclinations of less than 10 degrees however, not much correction is needed. This is also supported by wind tunnel testing conducted by Leasley et al [15]. Since the subsequent MAV flight testing was to be carried out without any direct flow inclination sensor, it was decided that the flow inclination encountered during the propeller testing was actually positive since it would be fairly representative of the angle of attack vs. flight speed the MAV would experience in flight. It was therefore decided not to make any corrections regarding the flow inclination. A correction was however made for the drag created by the motor and motor mount. This was done by measuring the drag of the motor without any propeller mounted and then subtracting this from the data. The total thrust as a function of rpm and velocity is shown in Figure 5 together with a Matlab-generated surface fit.

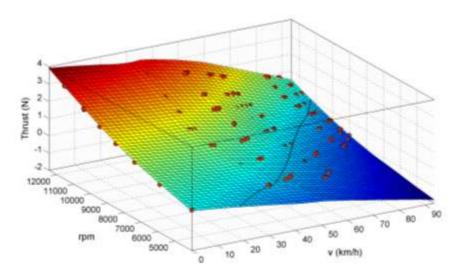


Figure 5. Logged propeller thrust plotted against rpm and velocity.

The measured data of thrust and torque were recalculated to thrust and power coefficients. It was seen that within the range over which the propeller would operate in flight, the propeller performed consistently with little Reynolds number effects. Only at the lowest tested speed, and in static testing, were the thrust and power coefficients seen to have some degradation. The resulting curves, plotted for each velocity, are shown in Figure 6. As a reference, the Reynolds number in these tests spans from 23,000 to 56,000, based on the blade chord at 75% of blade radius and with a velocity defined as $v_{Re} = \sqrt{v^2 + (\Omega R_{0.75})^2}$. These points correspond to the lowest rpm of the lowest speed and the maximum rpm of the highest speed, which both lies at approximately J=0.8.

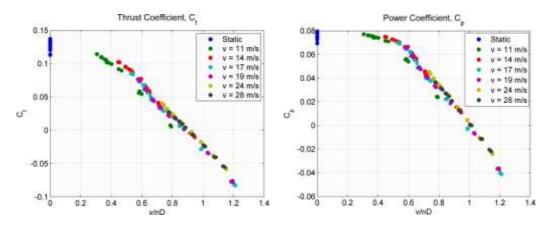


Figure 6. Thrust and power coefficients of APC 6x5.5 from propeller testing.

Based on these results, a Matlab surface fit model was created that was used for drag determination.

3. FLIGHT TESTING

The objective of the flight testing was to determine lift to drag characteristics of the MAV for different wind conditions, using the experimental propeller data. This means that any observed difference in aerodynamic properties due to variations in atmospheric turbulence cannot be distinguished whether it is derived from changes in the vehicles aerodynamics or propellers performance. It is nevertheless representative of any performance variation due to turbulence which was the purpose of the study.

3.1 Equipment

The aircraft selected for the flight test is an in-house designed Micro Air Vehicle called PingWing (Figure 7), originally developed for the 2007 US-European MAV competition [16]. The PingWing has been proven to perform well in very high winds and has forgiving flight characteristics in turbulence. The specifications of the PingWing MAV are summarized in Table 1.



Figure 7. PingWing MAV

PingWing Specifications					
Span (mm)	405	Motor	Mfly 180-08-15		
Length (mm)	370	Propeller	APC 6x5.5		
Takeoff Weight (g)	360	ESC	YGE 8s		
AR	1.5	Battery	TP G6 Pro-Lite 3s 1350mah 25C		
S (m ²)	0.110	Airfoil	MH 62		

Table 1. Specifications of PingWing MAV.

For this particular test the PingWing was equipped with an Eagletreesystems *elogger V4* data logger, complemented with additional Eagletreesystems sensors for measuring airspeed, altitude, GPS, 3-Axis acceleration and air temperature. No autopilot was used and all piloting was done under manual control. The logging frequency was set to 50 Hz.

3.2 Test Procedure and Data Analysis

The testing consisted of flying the MAV in a fixed pattern of as long straight lines as possible followed by gentle 180 degree turns. After take-off the pattern was entered at full throttle, which was then gradually decreased in small arbitrary steps until the airspeed no longer allowed the altitude to be maintained. For each throttle level, the aircraft was flown for two laps in the pattern. Once the lowest possible throttle to remain at altitude was reached, the throttle was increased but with a nose high attitude in order to further reduce the flight speed.

The flights were taking place in a relatively flat landscape. To give some sort of description of the terrain of the test sites, the Davenport classification scheme [17], as summarized in Table 2, has been used. The Davenport classification was developed in the discipline of wind engineering and has previously been used by Watkins et al [4] to classify the environment of MAVs.

#	Category	Roughness length z ₀ (m)	Landscape Description
1	Sea	0.0002	Featureless flat plain with a free fetch of several kilometres
2	Smooth	0.005	Featureless land surface without any noticeable obstacles and negligible vegetation
3	Open	0.03	Level country with low vegetation and isolated obstacles separated by min. 50 obstacle heights
4	Roughly Open	0.1	Area with low crops. Occasional obstacles with min. separation of 20 obstacle heights.
5	Rough	0.25	Crops of varying height. Scattered obstacles with separation of 12-15 obstacle heights.
6	Very Rough	0.5	Intensively cultivated landscape, many large obstacle groups with sep, of about 8 obstacle heights
7	Skimming	1.0	Landscape regularly covered with similar size obstacles (forest, suburb)
8	Chaotic	>2.0	City centres with mixture of low-rise and high-rise buildings, or large forests of irregular height

Table 2. Davenport classification of effective terrain roughness.

Some of the sensor data were somewhat noisy and seemed to be affected by electric noise. This included the throttle signal, rpm, and current measurements. As a first step, a 50-point moving average smoothing was applied to the data. An automatic screening was then, similarly to the propeller testing, made to sort out time frames where the data was considered valid for further analysis. By valid data denotes that the MAV was to be in level flight without any significant variation in altitude, throttle, or GPS heading. Instinctively, it may seem as if there should have been a requirement concerning variation in airspeed so that any acceleration after a turn is filtered out, but strong variations in airspeed in turbulent conditions made any such filtering impossible. On the other hand, it was found that the reduction in airspeed during turns was very small, and in combination with the data from the long straight passes that followed would barely influence the results. An example of flight trajectory is shown in Figure 8, where the valid time frames are marked in green.

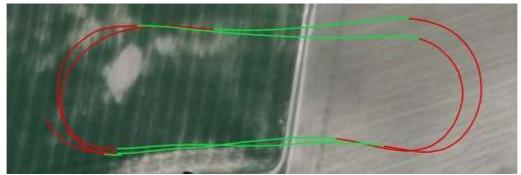


Figure 8. Example of flight trajectory used in testing. The green color marks segments of valid data.

For the data in the valid time frames, lift and drag coefficients according to Equations (4 - 5) were calculated for each data sample. The data was then averaged for each second, creating a smaller data set that could be illustrated and plotted more easily. A second data set was also created where the raw data was averaged for each step in throttle used during flight test, from full throttle down to minimum required throttle to stay flying. These averaged points were finally used to curve fit the lift to drag equation according to Equation (6).

$$C_L = \frac{L}{\frac{1}{2}\rho v^2 S} \tag{4}$$

$$C_D = \frac{D}{\frac{1}{2}\rho v^2 S} \tag{5}$$

$$C_D = C_{D_0} + C_{D_i} = C_{D_0} + AC_L + BC_L^2$$
 (6)

In Equation (4), Lift, (L) is always considered to be equal to weight (mg) and in Equation (5), drag (D), is equal to thrust (T) according to Equation (1).

4. RESULTS

Flights were made on several occasions and with varying wind conditions. In order to illustrate the differences between turbulent and calm conditions, this paper presents the results from the extremes: perfectly calm and extraordinary turbulent. All flights were conducted during November and in similar conditions in terms of pressure and temperature. In all tests, the sky was overcast and there was no noticeable thermal activity. In all, the results from three flights are presented.

• Flight1: This flight was conducted in pretty much as ideal conditions as they can ever be. The wind was exceptionally calm. The ground based wind meter at the site reported 0 m/s although flight data revealed a slight breeze of approximately 1.5 m/s at altitude. Temperature was 8°C, humidity 82% and air density 1.26 kg/m³. This kind of calm wind conditions and total lack of thermal activity rarely occurs. The terrain of the test site should according to Table 2 be defined as #4 "Roughly open". The results from this flight should be considered as a reference of the most forgiving ABL conditions possible.

- Flight 2: This flight was conducted at a day of high winds and at the same location as flight 1 (Davenport #4). The on-site wind meter reported 9m/s with gusts of up to 12 m/s. This can be regarded as an approximate upper wind speed limit for operation of MAVs. Temperature was 8°C with a humidity level of 80% and air density of 1.23 kg/m³. The flight was conducted in long straight passes aligned with the head- and tail-wind respectively. The altitude of the flight was approximately 40 meters above the ground. The conditions of this flight should be considered rough but as to be expected at these wind speeds.
- Flight 3: Flight 3 was conducted on the same day as Flight 2 but at a different location that generated more turbulence. This location should be described as a 7 on the Davenport scale. The site was situated next to a forest and with the wind direction perpendicular to the trees ridge line. The flying was conducted parallel to the ridge line on the leeward side in order to attain maximum turbulence. An approximate wind speed as acquired from flight data was 7-8 m/s at the flight altitude of around 1-1.5 times the trees' height. This generated a massive amount of turbulence to a degree that should be considered unrealistic in normal flight. Temperature was 8°C, humidity 85% and air density 1.23 kg/m³.

For each of the above flights the data was treated as described in the previous paragraph. Figure 9 illustrates the results from each of these flights. The multi-colored point clouds represent the one second averaged data. This illustrates the spread of the data for the different flights. The color is used to distinguish at which throttle level the data points were gathered. The green data points represent the total average for each throttle level. The black lines represent the curve fit of the data points. Finally, the curve fits for each of the three flights are compared in the lower right graph.

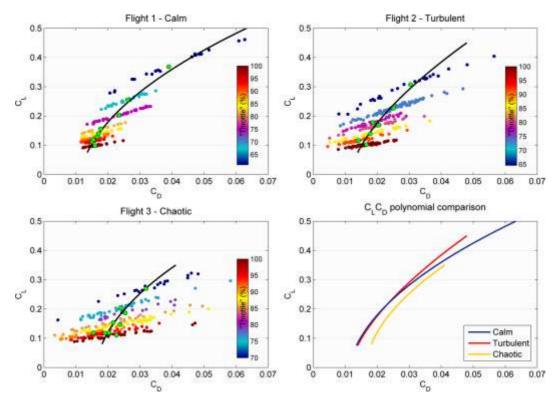


Figure 9. Data log result from each test flight. The scatter points represent one second averaged data and is colored based on throttle position. The larger green dots represent the average for each throttle level. The black curves are the polynomial fit of C_L vs C_D . Lastly, in the lower right figure, the polynomial fit of each flight is compared.

Since there were no major difference in temperature and pressure between the three flights, the

results are suitably illustrated by plotting the raw data of airspeed and propeller rpm (Figure 10).

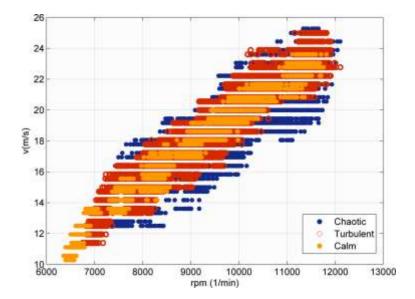


Figure 10. Raw data of airspeed as a function of propeller rpm.

The results show that even though the turbulence in Flight 1 and Flight 2 is at the opposite ends on the scale of practically occurring turbulence in MAV flight, the resulting lift to drag, averaged over time, is close to identical. This is the reason why only the results from the extremes are presented.

The results raised some questions about the validity of the data. It was very clear that the same rpm generated virtually the same indicated flight speed but uncertainties were if the airspeed was incorrectly measured for the turbulent flight, or if the energy required to turn the propeller at the same speed would be different for the turbulent condition. To validate the pitot tube measurements, the airspeed for each throttle level was compared to the GPS speed averaged for both up and down wind flight. This was done for the entire velocity range in both Flight 1 and Flight 2. The result indicated no difference in the airspeed measurements. For Flight 3, "chaotic", it was not possible to validate the pitot tube measurement; the result from Flight 3 therefore has less credibility but is included as a reference that nothing drastic happens even at unrealistic turbulence levels. The power to the motor was included in the data log and comparisons between the three flights revealed no measurable difference in power to rpm.

To illustrate the magnitude of turbulence, the Z-axis accelerometer data for a segment of straight and level flight from each of the three flights are given in Figure 11. As a reference of accelerometer noise due to motor vibrations or possible electronic noise, the top left chart shows accelerometer data of static testing with the MAV suspended horizontally on flexible wires and with the motor running at full speed.

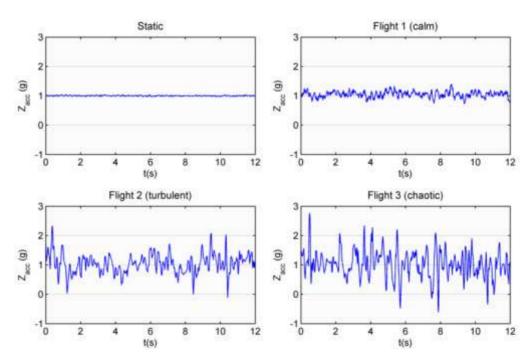


Figure 11. Z-axis accelerometer data of the three flights.

Considering the 50hz log frequency and the fact that the response time, or filter properties, of the Eagltree accelerometer unit is unknown, these data can only be seen as an indication of the fluctuations in angle of attack. Higher frequencies and larger peaks may exist but fail to be recognized by the logging equipment. It is interesting to note that even for the percieved calm air there is still some vertical movement. From the pilot perspective, not the slightest occurrence of wind or turbulence was noted. The air felt completely "dead" and no roll or yaw dirturbance, typical of turbulence, was seen in the MAV. In order to further illustrate the influence of turbulence on the MAV, complete 3-axes accelerometer data from a longer sequence of Flight 2 is given in Figure 12.

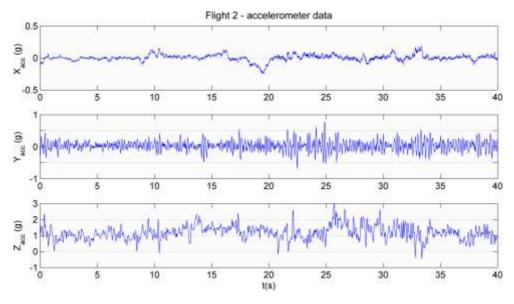


Figure 12. 40 seconds of 3-axis accelerometer data from Flight 2, at a velocity of 22 m/s.

The most noteworthy of these data is the magnitude of the Y-axis accelerations, illustrating the

significant oscillatory disturbances that occur around the yaw axis. This is typical of MAVs where the short distance between center of gravity and vertical stabilizer provides low yaw damping. From the pilots perspective this is seen as a constant excitation of yaw oscillations, similar to Dutch roll, which never sees enough smooth air to dampen out.

4.1 Complementary Testing

The focus of the flight testing was to compare the aerodynamic properties between different turbulence levels; however, the instrumentation in the MAV allowed some other interesting results to be extracted. In the above presented result lift to drag data is compared only down to the flight speed of minimum required power. Below this speed, the power required increases, but for the turbulent flights it was impossible to acquire reliable data in this low speed region. The entire lift to drag envelope was however tested for the calm flight where the MAV easily could be flown undisturbed at high angles of attack. Out of curiosity, the MAV was also flown the test sequence inverted. This would give some indication of the airfoil's impact on performance. The results over the complete operating range, including inverted flight, are shown in Figure 13. The figure includes data points averaged for each throttle level, as well as a $C_L C_D$ curve fit. For the purposes of comparison, the negative C_L curve is also mirrored to the positive side, illustrated by the faint grey line.

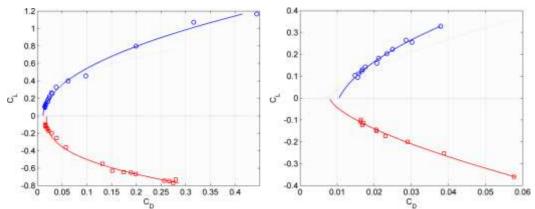


Figure 13. Total lift to drag characteristics including inverted flight. The left figure displays the entire operating range. The right figure displays the data in the range between full power down to minimum power required.

Interestingly for full power, as well as typical cruise speed, there is barely any difference in performance between inverted and upright flying. At lower speed, however, the inverted performance was degraded with increasing drag and lower C_L max.

In the current testing no correction of lift and drag has been made to account for the effect of tilting trust vector as angle of attack increases. This is because it is very difficult to measure angle of attack of a MAV in flight. Since MAVs, due to their compact geometry and low aspect ratio, greatly affect the adjacent flow field, a flow inclination device to measure the free stream angle cannot be installed. It would, however, be interesting to have some quantifiable measure of within what angle of attack range the MAV was operating. The PingWing was equipped with a 3-axis accelerometer. As long as the aircraft remains in straight and level flight without any significant turbulence, the relationship between the x- and z-axis accelerometers should provide a decent value of angle of attack. This was tested in calm wind and for positive angle of attack. The result, averaged for each step in throttle, is shown in Figure 14.

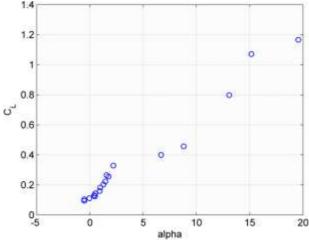


Figure 14. Lift coefficient as a function of angle of attack as acquired from accelerometer measurements.

Due to the previously mentioned uncertainties in the accelerometer data, the results should be interpreted with caution. The result however indicates that the MAV has an upper angle of attack limit of approximately 18-20 degrees. Some nonlinear behaviour appears to occur for lower angle of attack, while seen over the entire envelope the relationship is close to linear.

Another interesting complication with MAVs, compared to larger aircraft, is that the propeller slipstream covers a larger percentage of the wing area. This influences the wings' aerodynamics and potentially helps to delay stall. To investigate this behavior on the PingWing, the stall speed was tested both with power on as well as with motor powered off. In the latter case, the MAV was fitted with a folding propeller and the testing was conducted by flying at max speed, stopping the motor and gliding at constant altitude until the nose dropped due to stall. The accelerometer data helped identify the exact time of the stall in the data log. This was repeated several times in order to acquire a mean value. The result is presented in Table 3.

Table 3. Propeller slipstream effect on $C_{L max}$.

State	Vstall (m/s)	C _{L (L=mg)}	AoA (degrees)	C _L corrected
Power on	6.7	1.16	18	1.02
Power off	7.8	0.85	-	

It should be mentioned that the power off stall speed is conservatively read from the data in order to compensate for any possible lag in the pitot system. For the power on case, the C_L was corrected for the inclination of thrust vector using the crude angle of attack measure calculated from the accelerometer data. Clearly, the propeller slipstream has a positive effect on maximum lift.

5. DISCUSSION

The results of the flight testing have provided interesting data. The data indicates that varying turbulence intensities within the ABL have little to no effect on MAV performance. This was unexpected. When observing the MAV flying in the wind, it was seen to be violently thrown around and substantial control inputs were constantly required to maintain the flight path. The instinctive feeling was that the abuse from the turbulence would notably reduce the MAV performance. The results from Flight 2 show that for the range of turbulence in which it would be realistic to operate, it is not possible to measure the difference in performance. For higher C_L , it even appears as if the performance is slightly increased in turbulence, although this is probably within the error margin of the measurements. For the chaotic turbulence along the ridge line in Flight 3, the performance did decrease but since the airspeed measurements cannot be guaranteed and the turbulence level is not representative of any realistic scenario, that result is of less importance.

Several interesting conclusions can be drawn from the results. Looking at the accelerometer data in Figure 11, it is clear that the flow fluctuations occur at a rate where the aerodynamics are to be classified as unsteady. One way to quantify the degree of unsteadiness in an airstream is the reduced frequency parameter, $k=\omega c/2v$, where ω is the angular frequency of the fluctuating airstream, c is the chord of the wing and v is the free stream velocity. According to Leishman [18], the unsteady aerodynamic effects can generally be ignored for reduced frequencies in the range of 0 < k < 0.05. Above this limit the flow is to be categorized as unsteady. Furthermore, at reduced frequencies of 0.2 and above, the aerodynamics are to be considered highly unsteady and unsteady effects will begin to dominate the air loads. If a spectral density analysis is made of the accelerometer data of the most relevant case, Flight 2, it is seen that the most significant fluctuations occur in the range of 5 Hz. This corresponds to k=0.21, i.e. highly unstable. With this in mind, it is surprising that no difference in performance was noticed. On the other hand, the classification using reduced frequency does not account for the amplitude of the fluctuations, which reasonably should also play an important role. The vertical acceleration of Flight 2 is at maximum fluctuation between 0 and 2 g. At a speed of 22m/s this corresponds to a C_L variation of 0-0.22, or an angle of attack variation of 4.1 degrees, following the result in Figure 14. This variation in angle of attack is not excessive and is probably not enough to alter the vehicle's drag characteristics significantly by itself.

An interesting comparison can be made by assuming steady aerodynamics and simulating the potential drag increase in turbulence using the logged accelerometer data. This was done for Flight 2 and the accelerometer data in Figure 12. As a reference of lift to drag characteristics in steady flow, the result from the flight in calm air was used. Averaged over all data points this resulted in an increase in drag coefficient of 2.3%. This would hardly be noticeable in the data log. In this calculation, however, no account has been taken of the drag induced by the relatively large side forces caused by the turbulence. The induced drag due to side force is difficult to predict. A conservative estimate can be made by assuming that all of the side force is generated by the vertical stabilizers and then using standard equations for lift induced drag to compute the side force induced drag. The vertical stabilizer is a clean aerodynamic surface and should provide a much better "side force to drag ratio" then the actual vehicle has; these estimates should therefore be seen as the minimum drag increase. Based on the Y-axis accelerometer data from Figure 12, this approximation resulted in an average drag increase, due to fluctuating side force, of 12%. In total, if steady aerodynamic theory were valid for turbulent conditions, the average drag coefficient of Flight 2 should at a minimum be 14.3% higher than for Flight 1. This is for the flight velocity of 22 m/s and would increase further for lower velocities. Clearly, this would have been seen in the data and thus the unsteady aerodynamic effects do seem to be in effect. What is interesting it that it appears as if the unsteady effects benefit the MAV to the point that the drag generated by the constant disturbance in attitude and flight path is offset by an energy gain from the turbulence. The reason for this result is not completely clear and leaves room for speculation.

The possibility to extract energy from an oscillating airflow was first demonstrated in experimental measurements by Katzmayr [6]. Later analysis by Phillips [19] and Ribner [20] theoretically supports Katzmayr's results, but points out that for the turbulence levels found in the atmosphere the potential energy gains are very limited. Phillips estimates a manned glider aircraft to potentially see a thrust increase of approximately 10-20% of its drag, but also notes that in reality no performance gains in flight through turbulence have been observed. For a MAV flying in the ABL, the turbulence is comparatively stronger and, as pointed out by Langelaan and Bramesfeld [22], it opens up the possibility for greater energy gains according to Phillips' theory. More recent work has explored this possibility for smaller UAVs, of conventional wing tail configuration, either by using active control methods to optimally adjust the vehicles instantaneous angle of attack for maximum energy gain [21-23], or by tuning aeroelasticity and structural dynamics for the wing to naturally flex in order to optimally harvest the energy [24,25]. Another area of energy harvesting in atmospheric winds, which has some similarities to the energy gain in turbulence, is the phenomenon called dynamic soaring. Dynamic soaring can be described as energy extraction by cyclic maneuvering between layers of different wind speed within the earth boundary layer. It is an active research area that shows potential to substantial energy gains for small UAVs [26-28]. In the case of the PingWing MAV, it appears as if it passively manages to exploit energy from turbulence.

If passive energy gain from turbulence is possible purely from the MAV's aerodynamic shaping, it opens up a new perspective on MAV design and leads to many related research questions. How should a MAV be optimized in order to best perform in the turbulent environment of the real world? There may for instance be conflicting requirements between optimizing for low Reynolds numbers and optimizing for energy gain in turbulence. At lower Reynolds numbers, thin airfoils perform better, but on the other hand propulsive effects in turbulence are greater for thicker airfoils [6]. Can traditional stationary theory be used for MAV design? The present results are inconclusive. On the one hand, they show that stationary aerodynamic theory should not apply for flight in the turbulent environment of the ABL while on the other hand, on the tested MAV, the net effect of turbulence is negligible compared to the flight in smooth air. How general would this result be on other MAV platforms? A further interesting study would be to compare wind tunnel measurements with flight test data, as even in the calmest of conditions there is still some fluctuating wind within the ABL. Would the degree of static stability influence the performance in turbulence? A neutrally stable aircraft is in general considered the best for a sensor platform in the sense that its attitude (pitch, roll yaw) will be minimally impacted by turbulence. On the other hand, a MAV of flying wing configuration has very low pitch inertia and if longitudinally stable it will to some extent self-orient itself with the direction of the flow, which probably influences the possibility to gain energy from turbulence.

In the presented results no error margins have been included. The measurement error can be divided into two types: the sampling error and bias error. The sampling error was calculated assuming a normal distribution of the data points. In order to compensate for the noisy measurements in the turbulent flight, a significant number of data points were used to form the mean value and due to this the error analysis gave 95% confidence bounds that were so small that it did not make any sense to include them in the plots of the results. The bias error could have been estimated but since the data is of a comparative nature it would not contribute to the end result. Looking at the spread of the data, there are however some obvious uncertainties as regards the mean values. These errors are likely due to the stochastic nature of the ABL, or piloting precision, and these errors are very hard to estimate. The instantaneous performance could be seen to both improve and decrease due to the turbulence and this variation probably did not follow a normal distribution within the time frame of the measurements. The precision in the polynomial curve fits is also dependent on the number of points included, as well as their spread. For this reason, a more systematic method of setting the throttle levels, other than letting the pilot arbitrarily do the control, would have been better.

The described method of testing propellers is only peripheral to this work, but it has been very successful and deserves some discussion. Overall, the method has given very good results. It is an excellent wind tunnel substitution at a fraction of the cost. A drawback of the method is obviously that testing can only be carried out when the weather allows it. A benefit is that the environment is more representative then the one found in a wind tunnel and no correction for wall interactions etc. is needed. Experience shows that care should be taken to carry out the testing on a road aligned with the wind direction even if conditions are close to calm. The described test rig has worked well but could be further improved. The chosen data logger suffers from low sampling rate. A higher logging frequency would shorten the time needed for each test run. To minimize the problem of flow inclination not always being perpendicular to the propeller disk, the entire measuring rig could be made to swivel on the tripod similar to a weather vane. On the other hand, the non-zero flow inclination experienced with the rigid solution can also be used to advantage. In combination with the automated data reduction technique, a large amount of testing could fairly easily be done to build a database of propeller characteristics, where flow inclination is included as a parameter in addition to rpm and advance ratio.

6. SUMMARY AND CONCLUSIONS

A MAV was flight tested in varying wind conditions in order to investigate the effect of turbulence on performance. As a first step, the thrust and torque characteristics of the MAV's propeller were determined in a test rig carried on top of a moving car. The propeller data was then used to determine the drag characteristics of the MAV flown in calm as well as highly turbulent

wind. Surprisingly, the lift to drag ratio averaged over time exhibited little noticeable variation for the different turbulence levels. The MAV was highly impacted by the turbulent wind, which resulted in a constantly disturbed flight path as well as significant oscillations in yaw. If stationary aerodynamic theory is assumed this should have resulted in a noticeable increase in drag, yet performance was not affected. This indicates that the MAV to some extent benefits from the turbulence to the point that the increased drag due to interference is offset by an energy gain from the turbulence. Moreover, accelerometer data of the flight confirms that the flow around a MAV flying in the lower region of the atmospheric boundary layer is dominated by unsteady aerodynamic effects.

REFERENCES

- Kaimal, J.C. and Finnigan, J.J., Atmospheric Boundary Layer Flows: Their Structure and Measurement, Oxford University Press, 1994.
- [2] Stull, R.B., An introduction to boundary layer meteorology, Kluwer Academic Publishers, 1988.
- [3] Liu, H., Wind Engineering: A Handbook for Structural Engineers, Prentice Hall, 1991.
- [4] Watkins, S., Thompson, M., Loxton, B. and Abdulrahim, M., On Low Altitude Flight Through The Atmospheric Boundary Layer, *International Journal of Micro Air Vehicles*, Volume 2, Number 2, June 2010, pp 55-68.
- [5] Sytsma, M.J. and Ukeiley, L., Low Order Turbulence Modeling Methods for MAVs Flight Environment, AIAA Atmospheric Flight Mechanics Conference, Toronto, Ontario Canada, Aug 2010.
- [6] Katzmayr, R., Effect of Periodic Changes of Angle of Attack on Behavior of Airfoils, NACA-TN-2371, 1922.
- [7] Watkins, S., Loxton, B.J., Milbank, J., Melbourne, W.H. and Abdulrahim, M., Wind-Tunnel Replication of Atmospheric Turbulence with an Emphasis on MAVs, 46th AIAA Aerospace Sciences Meeting and Exhibit, Reno, NV, USA, Jan 2008.
- [8] Amadori, K., Lundström, D. and Krus, P., Automated Aesign and Fabrication of Micro-Air Vehicles, Accepted for publication in *Journal of Aerospace Engineering, Proceedings of the Institution of Mechanical Engineers Part G* [PIG], DOI: 10.1177/0954410011419612, 2011.
- [9] Lundström, D., Amadori, K. and Krus P., Automation of Design and Prototyping of Micro Aerial Vehicles, 47th AIAA Aerospace Sciences Meeting and Exhibit, Orlando, FL, USA, Jan. 2009.
- [10] Ostler, J.N., Bowman, W.J., Snyder, D.O. and McLain, T.W., Performance Flight Testing of Small, Electric Powered Unmanned Aerial Vehicles, *International Journal of Micro Air Vehicles*, Volume 1, Number 3, November 2009, pp 155-171.
- $[11] \quad UIUC\ propeller\ database:\ www.ae.illinois.edu/m-selig/props/propDB.html.$
- [12] Lundström, D., Amadori, K. and Krus P., Validation of Models for Small Scale Electric Propulsion Systems, 48th AIAA Aerospace Sciences Meeting and Exhibit, Orlando, FL, USA, Jan. 2010.
- [13] Gracey, W., Measurement of Aircraft Speed and Altitude, NASA Reference Publication 1046, Langly Research Center, Hampton, Virginia, USA.
- [14] DeYoung, J., Force and Moment Derivatives due to Propellers of Arbitrary Configuration Inclined With Respect To Free Stream, AIAA General Aviation Aircraft Design & Operations Meeting, Wichita, Kansas, USA, May 1964.
- [15] Lesley, E.P., Worley, G.F. and Moy S., Air Propellers in Yaw. NACA report No. 597.
- [16] Conte, G., Hempel, M, Rudol, P., Lundström, D., Duranti, S., Wzorek, M., Doherty, P., High Accuracy Ground Target Geo-Location Using Autonomous Micro Aerial Vehicle Platforms, AIAA Guidance, Navigation and Control Conference and Exhibit, Honolulu, HI, USA, Aug 2008.
- [17] Wieringa, J., Davenport, A.G., Grimmond, C.S.B. and Oke, T.R., New revision of Davenport roughness classification, Proceedings of the 3rd European & African Conference on Wind Engineering, Eindhoven, Netherlands, July 2001.
- [18] Leishman, J.G., Principles of Helicopter Aerodynamics, 2nd edn., Cambridge University Press, 2002.
- [19] Phillips, W.H., Propulsive Effects due to Flight through Turbulence, Journal of Aircraft. Vol. 12, No.7, 1975.
- [20] Ribner H.S., Thrust Imparted to an Airfoil by Passage Through a Sinusoidal Upwash Field, AIAA Journal, Vol. 31, No. 10, Oct 1993.
- [21] Depenbusch, N.T. and Langelaan, J.W., Receding Horizon Control for Atmospheric Energy Harvesting by Small UAVs, AIAA Guidance, Navigation and Controls Conference, Toronto, Canada, August 2010.
- [22] Langelaan J.W. and Goetz Bramesfeld G., Gust Energy Extraction for Mini- and Micro- Uninhabited Aerial Vehicles, 46th AIAA Aerospace Sciences Meeting, Reno, Nevada, USA, 2008.
- [23] Patel, C.K. and Kroo, I.M., Theoretical and Experimental Investigation of Energy Extraction from Atmospheric Turbulence, 26th International Congress of the Aeronautical Sciences, Anchorage, Alaska, USA, Sep 2008.

- [24] Ironside, D.J., Bramesfeld, G. and Schwochow, J., Modeling of Wing Drag Reductions Due to Structural Dynamics in Atmospheric Gusts, 28th AIAA Applied Aerodynamics Conference. Chicago, Illinois, USA, 2010.
- [25] Bramesfeld, G., Ironside, D. J., and Schwochow, J., Simplified Modeling of Wing-Drag Reduction due to Structural Dynamics and Atmospheric Gusts, AIAA 26th Applied Aerodynamics Conference, Honolulu, HI, USA, Aug 2008.
- [26] Boslough, M.B.E., Autonomous Dynamic Soaring Platform for Distributed Mobile Sensor Arrays, Tech. Rep. SAND2002-1896, Sandia National Laboratories, California, USA, June 2002.
- [27] Lawrance, N.R.J. and Sukkarieh, S., A guidance and control strategy for dynamic soaring with a gliding UAV, 2009 IEEE International Conference on Robotics and Automation, Kobe, Japan, May 2009.
- [28] Mears, M., Energy Harvesting for Unmanned Air Vehicle Systems using Dynamic Soaring, 50th AIAA Aerospace Sciences Meeting, Nashville, TN, USA, Jan 2012.